Characterisation of a resonating system by mean of electrical impedance measurements

L. Ausiello[1]

[1] School of Electrical and Mechanical Engineering, University of Portsmouth, UK

Abstract

In recent years the use of affordable alternatives to impact hammer measurements to assess musical instruments and systems with complex resonating behaviour has emerged. By using small electro-dynamic exciters, standard methodologies such as sine-sweep measurements and real time spectral analysis together with pink-noise have shown positive results to quickly and economically characterise both the mechanical and the mechano-acoustical responses of musical instruments and resonating plates. This investigation tries to expand on the theory behind the coupling of an exciter and a resonating structure. Electrical impedance measurements will be performed at the terminals of an exciter placed in different positions of an unknown soundboard. The interaction between the actuator and the plate will be interpreted drawing from the models describing the coupling between an electro-dynamic transducer and a vented enclosure. Accordingly, a lumped element model will be presented and discussed. The goal is to estimate which is the minimum number of measurements needed to characterise the first ten modes of an unknown structure. A criterion to select the correct size and power handling capability of the exciter used to sense will also be discussed.

1 Introduction

Quantitative measurements are standardised practice in the loudspeaker and microphone industry and markets [1, 2, 3], but in the compartment of musical instruments they are seldom provided. Past studies [4, 5] successfully employed the sine sweep method to gather the acoustic response of a guitar using small exciters. More recent research [6] consolidated the use of sine sweep to yield large frequency bandwidth measurements with high coherence values between the applied force and the corresponding vibrational or acoustic output of the Device Under Test ($\mathbf{DUT}$). The intrinsic repeatability and good accuracy of the method are paired with a low-cost setup consisting of electro-dynamic exciters, accelerometers or pressure microphones (if an anechoic environment is available).
This paper focuses on how impedance measurements on the actuator can be used to retrieve relevant data regarding the first resonance modes of the DUT even before performing vibrational or acoustic measurements. This article refers to published literature with regards to the scope and justification of the methodology [6], and presents two alternative models which explain what can possibly be sensed by the actuator placed on a spruce soundboard. Section 2 shortly recaps how the sine sweep is used with small exciters, with a reference unbraced board being measured by two electro-dynamic transducers. The following section 3 describes the influence of the exciter's position and electro-mechanical properties are addressed. A case study with soundboard of composite sustainable materials is presented live at the conference, while a final discussion of the presented results is given in Section 4.

2 Exciters and sine sweep for musical instruments measurements

The sine sweep method is extensively adopted in acoustics since it offers a wide frequency bandwidth [7, 8]. Uses of this techniques are prominent in room acoustics [9, 10, 11] due to its resilience to background noise and to the ability to separate the nonlinear harmonic distortion from the linear part of the spectrum. This latter feature allows using sources with a significant input gain exciting high-frequency modes. Firstly presented at RS2018 [4], an application of this technique to the measurement of an acoustic guitar was then expanded in [5], where it is shown that this approach is capable of capturing changes such as the presence or absence of the varnish on the guitar top, and alterations in bracing patterns in both the soundboard and the back of the instrument. In [6] four exciters were chosen and validated against the standard impact hammer technique. In this article data and measurements regarding two actuators will be shown (those with a total mass of approximately 12.5 g, and 50 g - including the wax or putty material used to position them on the

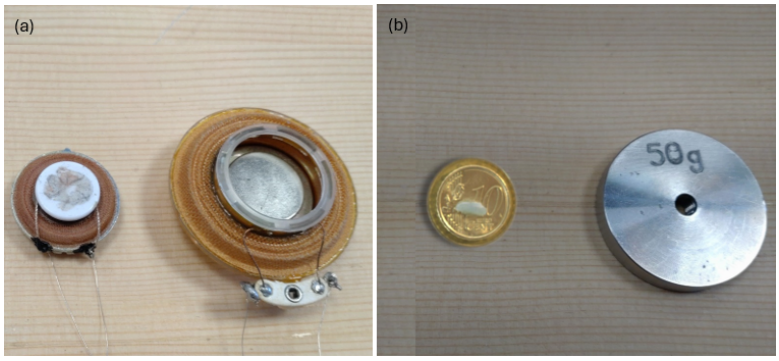

Figure 1: (**a**): The electro-dynamic exciters used in this work, from left to right: Exciter 3 (EXC_3), and Exciter 4 (EXC_4). (**b**): equivalent masses, from left to right: 12.5 g, 50 g.

	Tot. Mass (g)	Fs (Hz)	Re (Ω)	Qms	Qes	Qts	Cms ($\mathrm{mm\,N^{-1}}$)	Mms (g)	Rms ($\Omega\,\mathrm{m}$)	Bl ($\mathrm{N\,A^{-1}}$)	L10 (mH)
EXC_3	12.5	454	1.7	7.90	2.80	2.07	0.20	0.58	0.21	1.01	0.02
EXC_4	50	333	4.0	8.60	1.44	1.24	0.21	1.06	0.26	2.48	0.04

Table 1: Thiele and Small (T&S) parameters of two exciters, measured in free air.

plates), as per Table 1 and Fig. 1. The names used here are coherent with [6] to allow the readers to put both articles in relationship with each other.

2.1 Effects of small exciters on the acoustic response of raw, unbraced boards

An unbraced, raw spruce board of dimensions $600 \times 210 \times 4$ mm thick, is used to recap how a sine sweep measurement is done and analysed. The thickness of the board was measured on a matrix of 9 points using a gauge. The resulting 9 values were averaged, and the error was kept to the decimal point. Accordingly, a stated thickness of 4 mm corresponds to 4 mm +/- 0.1mm (this will be used throughout the paper). The frame used, visible in Fig. 2, is made of hard plexiglass, with a rectangular opening at the bottom to let the plate vibrate as a dipole, and a rectangular frame at the top to distribute the pressure provided by regularly spaced clamps. The mass of the bottom structure is 5.650 kg, while the one for the top rectangular bezel is about 380 g, for a total mass of more than 6 kg. In Fig. 2, **L1** and **C** indicate the locations of the excitation points, while **R1** is the position where an accelerometer was glued on the top surface of the DUT. Such locations on the board were chosen to minimise or maximise the impact of the actuators on the board, as will be discussed shortly.
For reference, we show here also the original measurement of the impact hammer used for the validation in [6]. The model is a PCB Piezotronics 086E80, while the accelerometer is a PCB Piezotronics 352C23.
The exciters, as stated before, were two small electro-dynamic actuators named **EXC_3**, and **EXC_4**, characterised by the Thiele and Small (T&S) parameters [12, 13, 14] in Table 1. Their dimensions are progressively larger, as well as their Bl and force factor (where l denotes the length of the conductor immersed in the magnetic flux density B), indicating a larger power handling capability and a higher efficiency in exciting the board. The actuators' T&S parameters were measured using the "added-mass" method [15].

2.2 Assessing the added exciter's mass

As addressed extensively in [6], one obvious question concerns the effect of the exciter's added mass on the collected IR. For each exciter, four configurations were used to assess this issue: first, the impact hammer technique was used on the raw board; second, the same impact hammer technique was used on the board augmented with a coin the same weight as the exciter; third, the impact hammer technique was used on the board augmented with the exciter; fourth, the exciter and sine sweep method was used. All throughout, the excitation point L1 was considered, and the accelerometer was located in R1 all the while. The two exciters from Table 1 were investigated, which led to two repetitions of the same experiment.
To collect reliable data, the miniature impact hammer measurements were averaged across five repetitions [4, 16]. Note that all impact hammer measurements throughout the paper were subjected to the same averaging procedure, but for brevity, this will not be stated further. The hammer and accelerometer signals were read by a

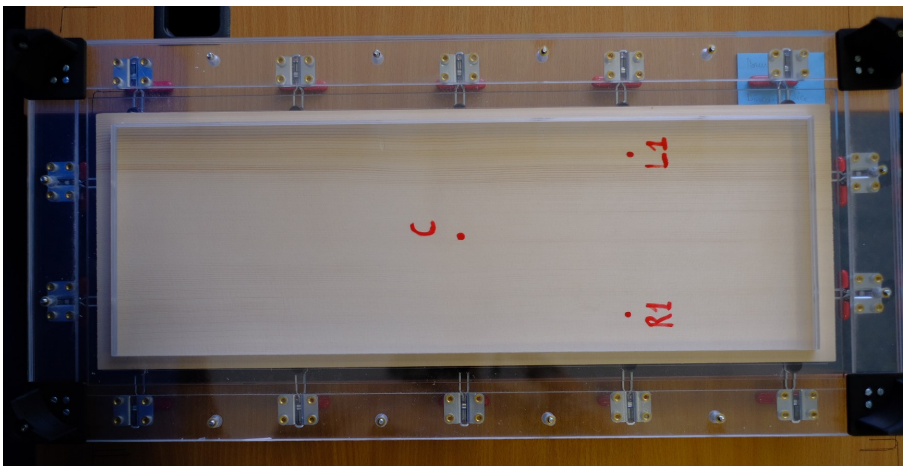

Figure 2: Schematic representation of the measurement setup. The red dots **L1** and **C** indicate the excitation points, namely locations for either the impact hammer hits or the contact point for the exciters while performing the validation measurements, while **R1** indicates the position of the accelerometer.

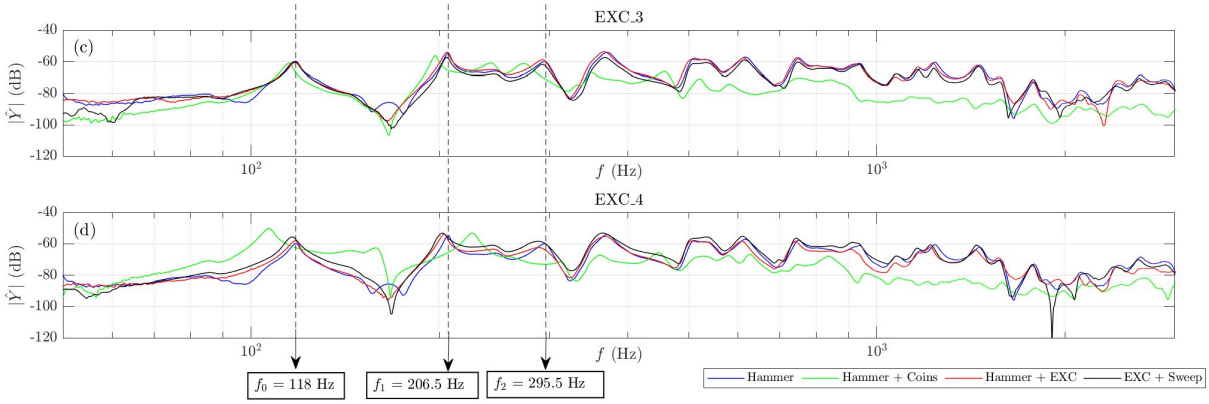

Figure 3: Exciter validation. For all panels, the spectra are as follows: hammer on raw board (solid blue); hammer on board plus exciter (red); hammer on board plus coin (green); sine sweep and exciter (black). The coins have the same mass as the exciters, as per Table 1. Input point in L1, readout in R1.

Zoom F8 audio interface, connected to Audacity to record multiple hits regularly spaced in time. The coins have masses of 12.5 g, and 50 g, the same as the two exciters as per Table 1. The signal chain driving the exciters consisted of a laptop with Adobe Audition 3.0 generating a $45 - 8000$ Hz sine sweep stimulus normalised at -6 dB LUFS, which was outputted by a Focusrite Scarlet 2i2 audio interface into a 20 W linear amplifier. Each stimulus contained two sweeps, ten seconds long, with a silence interval of 5 seconds in between. For all measurements, the sampling frequency was 48 kHz and the bit-depth was 24 bit [8]. The stimulus output voltage measured at the exciters' terminals was calibrated depending on the nominal impedance of each actuator to produce 0.25 W of power at 1 kHz. This was measured by a Fluke 177 multimeter at the exciter's terminals.

Frequency response functions (FRF) were computed dividing the cross power spectrum of the input and output measurements signals by the autopower spectrum of the input force of the hammer signal. The spectra are plotted in terms of the mobility Y in dB. Results of the two experiments are collected in Fig. 3, where the benchmark FRF gathered using the impact hammer is displayed as a solid blue line. The coin-mass and exciter-mass cases are shown in green and red, respectively, while the black solid curve represents the FRF acquired with the exponential sine sweep method.

The validation procedure conducted in [6] proved that using the excitation point C does not yield reliable data, because there is an interaction between the actuators and the first resonant mode of the board, as visible in Fig. 4. The presence of the transducers significantly affects the results in the lower range. Discrepancies are also evident between the coin-mass and exciter-mass cases. The coin behaves as a passive added mass, shifting frequencies downward. Conversely, the presence of the exciters causes an upward shift, suggesting a different behaviour. More insight into the relationship between actuators and DUT will be presented in the following section, which discusses electrical impedance measurements of the transducers.

To summarise, by choosing a more neutral measurement point, such as L1, the impact of the exciter on

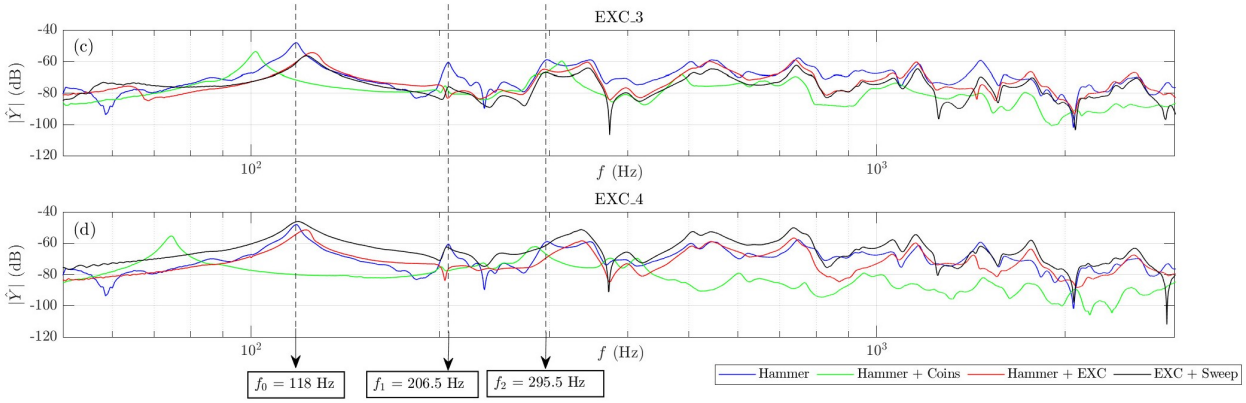

Figure 4: Exciter validation. Same as Figure 3, but excitation point in C.

		EXC_3	EXC_4
Hammer	f_0 (Hz)	117	116
$f_0 = 118$ Hz	dev. (%)	-0.85	-1.72
	dev. (cent)	-14	-29

Table 2: Frequency and relative deviations of first detected peak f_0 in the FRF spectra using the benchmark hammer measurement and the exciters.

unbraced boards can be made negligible, as shown. Table 2 summarises the estimation relative error when using either the impact hammer or any of the four exciters in position L1.

3 Assessing the exciters' impedance

Electrical impedance measurements performed on the exciters helped understanding and modelling the interaction between the electro-dynamic transducers and the board. Such measurements are considered standard procedure in electro-acoustics design, and the reader can refer to extensive literature if required [12, 13, 17, 18]. A Clio Pocket system by Audiomatica[1] was used for the impedance measurements. It was connected via a cable terminating with crocodile clips, which showed an internal resistance of $0.1\,\Omega$ +/- $0.05\,\Omega$. The actuators were wired using thin, light, and flexible wires. When an exciter was mounted on the board, its wires were bonded to the plexiglass frame visible in Fig. 2 with putty. A portion of each wire created a small arc, while the remaining portion after the putty was attached to a crocodile clip.
A preliminary statistical analysis measured EXC_3 in a single position (L1) 32 times. The actuator was repositioned on the board several times (using the same amount of wax), while small variations on its location or orientation were introduced to mimic a real-life scenario. The analysis showed that the single large impedance peak was located, on average, at $75.6\,$Hz, with a mean amplitude of $3.76\,\Omega$; three sigma corresponded to +/-2.7 Hz in frequency and +/- $0.57\,\Omega$ in amplitude. This suggested a good repeatability of the electrical measurements involved.
EXC_3 and EXC_4 were measured, and their impedance curves were recorded while located in both positions L1 and C, similar to the configurations used to capture the IR of the soundboard. Fig. 6 compares the two excitation points. Furthermore, a second experiment was designed to highlight the effects of adding mass to the exciters in both excitation points. Fig. 7 shows the results for EXC_3.

3.1 Modelling the electromechanical coupling

While in [6] a Reduced Order Model is presented first to explain the interaction between the exciters and the board, an explanation more in line with loudspeaker theory will be used here. The approach draws from a similar idea proposed by Lazar and Kubota in [19], and expanded by Magalotti et Alii in [20], thus using a similar lumped element circuit and symbols. Fig. 8 presents the electrical equivalent impedance $\mathbf{Z}_L(s)$ observed beyond the driver's voice coil.

[1] Audiomatica, `https://www.audiomatica.com/wp/?page_id=3557`

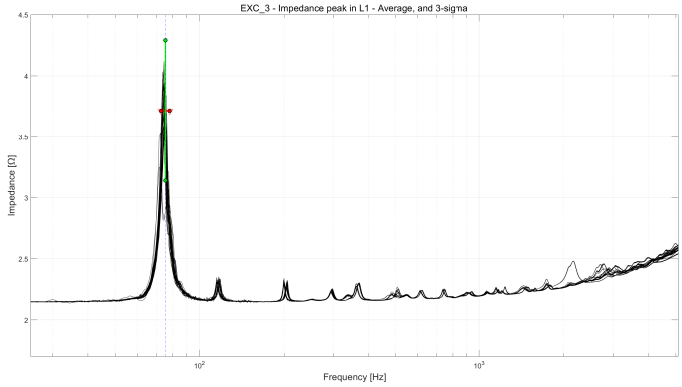

Figure 5: Statistical analysis of the electrical impedance of EXC_3 data measured in L1. 32 measurements were collected. The dashed blue line corresponds to the average value of frequency of the peak (75.6 Hz), the green line corresponds to +/- 3-sigma of the amplitude (+/- 0.57 Ω), while the red line corresponds to +/- 3-sigma of the frequency of the peak (+/-2.7 Hz).

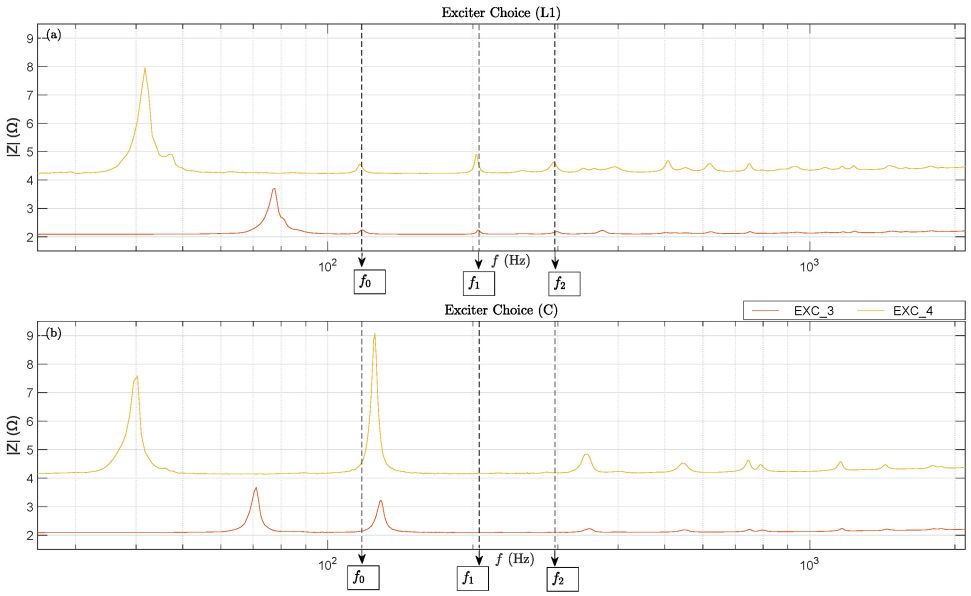

Figure 6: Electrical impedance plots of two exciters placed in L1 (panel (a)) and C (panel (b)). The dashed lines represent the first resonances of the board. In position L1, all curves present a single large peak followed by small local maxima. In position C, all curves show two large peaks and a different set of local maxima.

The original scenarios investigated in [19, 20] depicted the interaction between a loudspeaker driver and a vented cabinet, which creates a coupling of two resonating systems. In both cases, the series electrical resonator (highlighted in blue in Fig. 8) corresponds to a Helmholtz resonator, comprising oscillating air mass within a pipe. In the presented analysis instead, the coupling is between an exciter and one (or more) resonant modes of the plate being measured. Accordingly, the series resonator (in blue) is now modelling the fundamental mode $(0, 0)$ of the board to whom the exciter is coupled when located in position C. It is imperative to note that, like the cited studies, all losses have been neglected. Based on the analysis from [19], $\mathbf{Z}_L(s)$ can be expressed as follows:

$$\mathbf{Z}_L(s) = sL_1 \frac{1 + s^2 L_2 C_2}{1 + s^2(L_1C_1 + L_2C_2 + L_1C_2) + s^4 L_1C_1L_2C_2} \tag{1}$$

The two large impedance peaks visible in Fig. 7 (b) are caused by the two poles of the denominator of (1). Changing the variable from s to $j\omega$, and dividing by the coefficient of the s^4 term, (1) can be then rewritten as:

$$\omega^4 - \omega^2 \left(\frac{1}{L_1C_1} + \frac{1}{L_2C_2} + \frac{1}{L_2C_1} \right) + \frac{1}{L_1C_1L_2C_2} = 0 \tag{2}$$

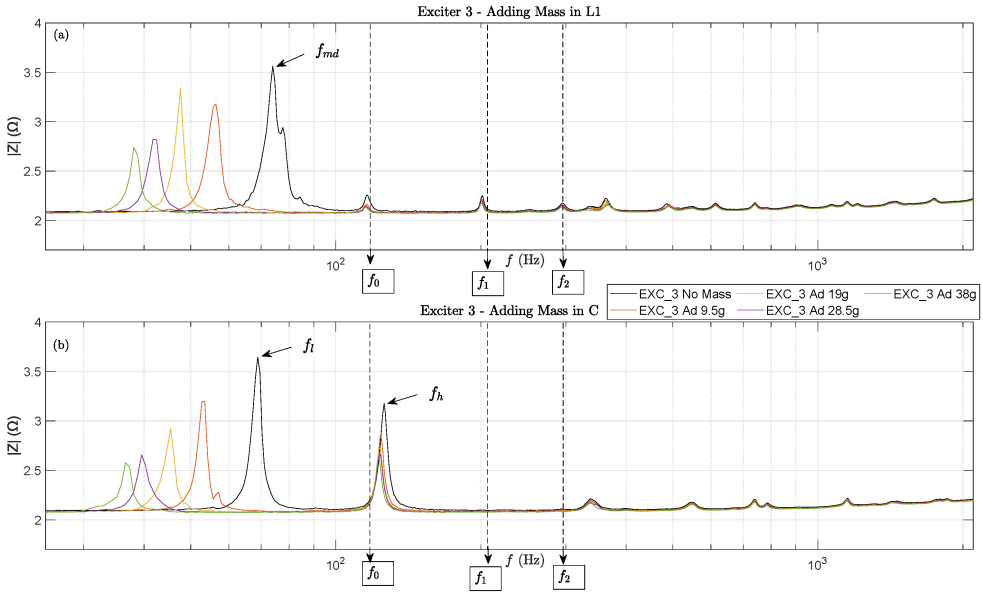

Figure 7: Electrical impedance plots of EXC_3 placed in L1, panel (a), and C, panel (b). Rigid masses are progressively added on the exciter to alter its mechanical resonance (f_{md}). The dashed lines represent the first modes of the board; mode $(0, 0)$ (f_0=118 Hz) is located near the first small local maxima in panel (a), and in between the peaks f_l and f_h ("low" and "high") in panel (b). A good excitation point (a) can be identified when a single peak f_{md} (resonance of DUT + transducer) is visible. When mass is added, f_{md} shifts down in frequency, while smaller local maxima of the curve are not affected.

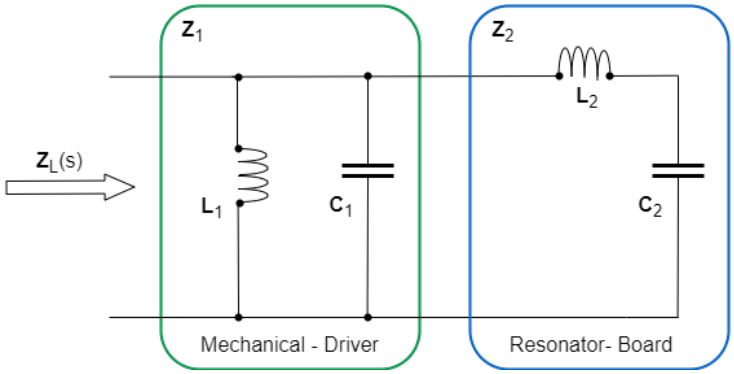

Figure 8: Electrical equivalent model [19, 20] of the system composed by an exciter (mechanica driver) coupled to a mode of the soundboard being measured (resonator)

.

After a few algebraic manipulations, one obtains [20]:

$$\omega_{md}^2 = \frac{1}{L_1 C_1}; \qquad \omega_b^2 = \frac{1}{L_2 C_2}; \qquad \omega_M^2 = \frac{1}{L_2 C_1}; \tag{3}$$

where ω_{md}^2 is the mechanical resonance of the driver, ω_b^2 is the first resonance of the board, and the subscript M could be intended as "Mix" or "Mutual", suggesting a dependency on both elements. Thus, (2) becomes:

$$\omega^4 - \omega^2(\omega_{md}^2 + \omega_b^2 + \omega_M^2) + \omega_{md}^2\omega_b^2 = 0 \tag{4}$$

The two solutions of the quadratic equations (4) can be called ω_l^2 and ω_h^2, using the same subscript for *low* and *high* as used in Fig. 7, and they can be written as function of ω_{md}^2, and ω_b^2, as:

$$\omega_l^2\omega_h^2 = \omega_{md}^2\omega_b^2 \tag{5}$$

Considering only positive frequencies, (5) can be rewritten as:

$$\omega_l\omega_h = \omega_{md}\omega_b \tag{6}$$

Summarising, when an exciter is located in L1, the system (DUT + actuator) can be seen as a loudspeaker in free air. When an exciter is attached in C, the system (DUT + actuator) can be seen as analogous to a

loudspeaker placed in a vented box, i.e. coupled with a resonator. The former scenario yields an impedance curve showing a single peak f_{md} as per Fig. 6 (a), while the latter produces data depicted in Fig. 6 (b), where two main peaks, named f_l, and f_h, are visible. Equation (6) suggests that, in essence, the geometric mean of the frequencies of two peaks in the impedance curve of the exciter positioned in C is equal to the geometric mean of the product of the exciter resonance frequency (when attached in L1), and the frequency of the first resonant mode (0 0) of the board.
Interestingly, the same scenario is described in the seminal paper by Thiele [12], more precisely in Fig. 5, pag. 385. In the reference the author states that between f_l and f_h a minimum called f_b can be identified, corresponding to the resonant frequency of the Helmholtz resonator (the vented box, hence the subscript *b*) to which a transducer is coupled. In the suggested analogy, the first resonant frequency of the board f_0 corresponds to f_b as used by Thiele, thus $f_0 = f_b$. If this notation is adopted, the relationship between these three impedance peaks and the resonant frequency of the loudspeaker in free-air f_{md} is presented in [13], Eq. (105), and can be written using frequencies instead of pulsations as:

$$f_{md} = \frac{f_l \cdot f_h}{f_b} = \frac{f_l \cdot f_h}{f_0} \tag{7}$$

A few more reflections are worth mentioning here. In [20] the authors use (6) to estimate the shift of the original mechanical resonance f_{md} of the loudspeaker, once the driver is installed in a vented cabinet. In the presented case, information about f_{md} is always available, when measuring a soundboard in position L1. On the contrary, f_b (or f_0) is not necessarily known unless an impact hammer measurement is concurrently done. This suggests that f_b can, in fact, **be estimated from impedance data**. From Fig. 6 (b) showing the impedance measurement in C, $f_l = 69$ Hz, and $f_h = 126$ Hz can be retrieved. From Fig. 6 (a), and the measurement in L1, the value $f_{md} = 74$ Hz can be found. By substituting in (7), f_b becomes:

$$f_b = f_0 = \frac{f_l\, f_h}{f_{md}} = \frac{69 \cdot 126}{74} = 117.4\,\text{Hz} \tag{8}$$

which is within the statistical variance mentioned at the beginning of section 3, and in agreement with the estimations summarised in Table 2 from both impact hammer and sine sweep data. It must be noted that the validity of lumped element models is limited to a low-frequency range [12, 13, 20], and care should be used elsewhere. These results show that excitation points can be assessed and verified using electrical impedance measurements. If, from measurement, the interaction between the transducer and the board appears negligible, it can be assumed that the actuator is correctly working past its mechanical resonance [21]. Small local maxima of the impedance curve may still be visible in the proximity of the eigenmodes of the DUT, as discussed in literature [21, 22]. The reader who wished to expand on the topic can also refer to the original ROM presented in [6], which is included in the Appendix.

4 Result analysis and comments

The use of small electro-dynamic actuators, driven by wide-band signals like sine sweeps or pink noise, allows the acquisition of reliable data when applied to guitar soundboards. In a benchmark test, two low-cost transducers returned data matching the benchmark provided by the impact hammer technique using expensive equipment. A robust method to identify an effective excitation point was explained based on impedance measurements. Through this method, one can effectively select exciters with appropriate power handling capabilities, dimensions, and bandwidth. With as few as two measurements, users can estimate the frequency of the first resonance of a DUT and verify the exciter's functionality beyond its mechanical resonance. Small local maxima in the impedance curve are expected near the eigenmodes of the DUT under such conditions.

5 Conclusions and future work

This study introduced an approach to assessing the spectral properties of guitar soundboards using small electro-dynamic actuators for wideband measurements. The results confirmed the reliability of the sine sweep method when compared to the conventional impact hammer technique, demonstrating its efficacy across a broad frequency bandwidth of up to 8 kHz. Moreover, the findings indicated that the sine sweep method, coupled with exciters of varying sizes, efficiently captured a wide range of acoustic responses, making it a versatile tool in musical instrument manufacturing.
A lumped element model was presented to explain the interaction between small exciters and an unbraced board, offering a robust means to select an appropriate excitation point and estimate the frequency of the first eigenmode of a device under test without prior knowledge of its vibrational behaviour. Future work will

expand the electrical equivalent model to extract more information from the DUT through electrical impedance measurements. Future research will explore the performance and reliability of low-cost piezoelectric sensors concerning the affordability of the measurement setup.

Appendix A

The experimental results can be understood by modelling the coupling between the board and the exciter. Furthermore, this model suggests that electrical impedance measurements at the exciter's terminals can detect compliant board peaks, which may affect the reliability of the measurement method. The coupled system is given as:

$$\rho h \frac{\partial^2 u(\mathbf{x},t)}{\partial t^2} = \mathcal{L}(u(\mathbf{x},t)) - 2\sigma\rho h \frac{\partial u(\mathbf{x},t)}{\partial t} + \delta(\mathbf{x}-\mathbf{x}_{md}) C_{ms}\left(w(t) - u(\mathbf{x}_{md},t)\right) - \delta(\mathbf{x}-\mathbf{x}_{md}) BlI(t) \tag{9a}$$

$$M_{ms}\ddot{w}(t) = -2M_{ms}\,\eta\,\dot{w}(t) - C_{ms}\left(w(t) - u(\mathbf{x}_{md},t)\right) + BlI(t) \tag{9b}$$

$$V(t) = L_e\dot{I}(t) + R_eI(t) + K(\dot{w}(t) - \dot{u}(\mathbf{x}_{md},t)) \tag{9c}$$

In the above, $u = u(\mathbf{x},t)$ is the displacement of the board, for coordinate $\mathbf{x} \in (0,L_x)\times(0,L_y)$ and time t; $w = w(t)$ is the displacement of the exciter. $I = I(t)$ is the current through the exciter, and $V(t)$ is the externally-supplied voltage.
In (9a), $\mathcal{L}(u)$ represents the differential operator associated with the orthotropic plate equation, not specified here for brevity. See e.g. [23] for an explicit form of such operator. Furthermore, in the above, $\mathbf{x}_{md}$ denotes the coordinate of the exciter's contact point on the board, which may be identified as C or L1.
Constants appear as: $\rho = 390$ kg $\cdot$ m^{-3}, the density of the board; $h = 4$ mm, its thickness. Furthermore, M_{ms}, C_{ms}, R_e, L_e, Bl are the Thiele & Small paramters of the exciter when attached to the board, and are summarised in Table 3.

	f_{md} (Hz)	R_e (Ω)	C_{ms} (mm N^{-1})	M_{ms} (g)	Bl (N A^{-1})	L_e (mH)
EXC_3	73.9	2.1	0.35	13.18	1.01	0.06

Table 3: Thiele and Small (T&S) parameters of EXC_3 when located in position L1. This configuration can be interpreted as a driver in free-air as intended in the works from Thiele, Lazar and Kubota, and Magalotti [12, 13, 19, 20]. A noticeable difference is visible in the value of the moving mass M_{ms}.

Finally, σ, η and K are, respectively, the loss coefficient of the board, the loss coefficient of the exciter when attached to the board, and a constant of back-electromechanical coupling. For brevity, only EXC_3 will be considered here. It is convenient to derive a reduced-order model (**ROM**) comprising the plate's first mode alone since this is the most influenced by the location of the exciter $\mathbf{x}_{md}$. To that end, for the sake of simplicity, it is assumed that

$$u(\mathbf{x},t) \approx \sin\frac{\pi x}{L_x}\sin\frac{\pi y}{L_y} q(t), \tag{10}$$

where the modal shape given here corresponds to the first mode of a simply-supported board, and where $q(t)$ represents the time evolution of the mode. The mathematical expression for the modal shape is justified as the first modal shape of the clamped board is "qualitatively" similar in that it presents a maximum at the plate's centre and progressively tapers off toward the edges. Inserting (10) in (9a) and performing a standard modal projection [24] leads to the reduced order system:

$$\ddot{q}(t) = -\omega_0^2 q(t) - 2\sigma\dot{q}(t) + bM_{ms}M^{-1}\,\omega_{md}^2\left(w(t) - bq(t)\right) - bM^{-1}BlI(t) \tag{11a}$$

$$\ddot{w} = -2\eta\dot{w}(t) - \omega_{md}^2\left(w(t) - bq(t)\right) + M_{ms}^{-1}BlI(t) \tag{11b}$$

$$V(t) = L_e\dot{I}(t) + R_eI(t) + K(\dot{w}(t) - b\dot{q}(t)). \tag{11c}$$

In the above, the modal weight was introduced as $b := \sin\frac{\pi x_{md}}{L_x}\sin\frac{\pi y_{md}}{L_y}$, quantifying the influence of the mode shape at the contact point. All parameters in the ROM are known or can be estimated easily. In fact, $\omega_0 = 2\pi f_0$, where $f_0 = 117$ Hz is the measured frequency of mode (0, 0) as given in Table **??** for EXC_3; $\sigma = 3\log(10)\tau_{60}^{-1} \approx 14$ s^{-1} is estimated from the board's approximate decay time for mode (0, 0) of $\tau_{60} \approx 0.5$ s, where τ_{60} is the time required for the energy to decay by 60 dB per mode [25]; the modal mass of the board for mode (0, 0) is $M = 0.25\rho h L_x L_y \approx 50$ g, as given by the modal projection; $\mathbf{x}_{md} := (x_e, y_e)$ is estimated from Fig. 2. For C one may take $\mathbf{x}_{md} := (0.5L_x, 0.5L_y)$, and for L1 $\mathbf{x}_{md} := (0.7L_x, 0.9L_y)$. $\omega_{md} = 2\pi f_{md}$, where $f_{md} := \sqrt{C_{ms}M_{ms}^{-1}}/2\pi = 73.9$ Hz as given in Table 3. η and K are guessed. Here, the following are used:

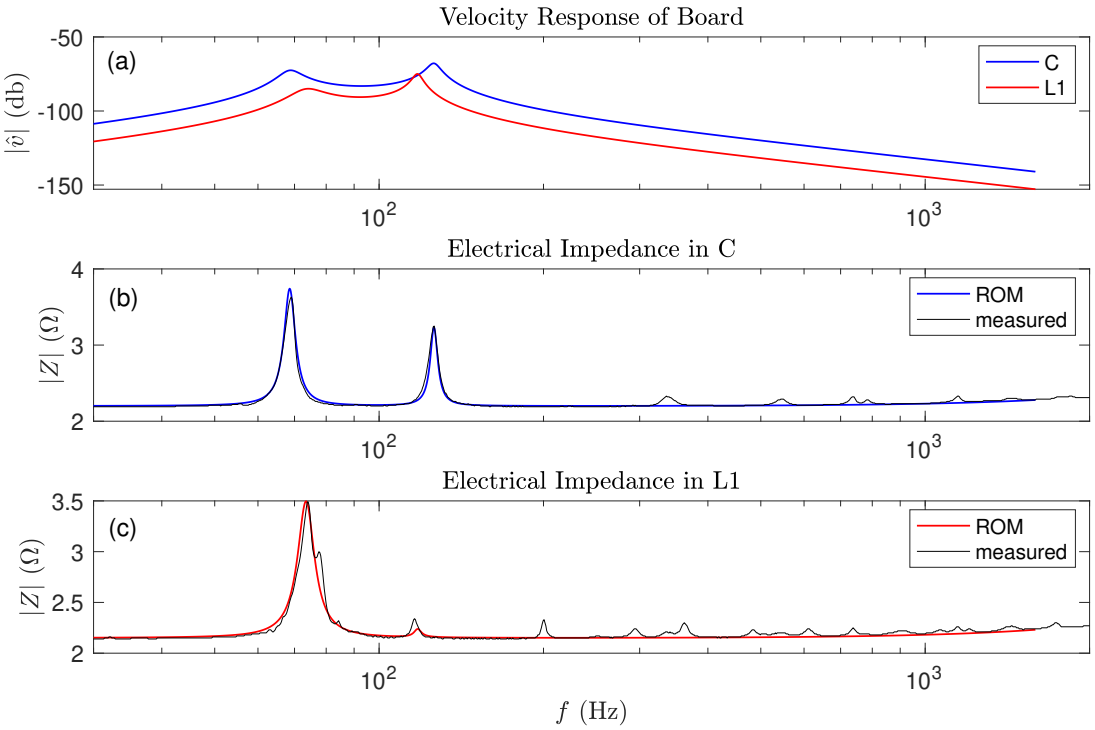

Figure 9: Reduced-order model (ROM) of the plate-exciter system for EXC_3. The stiffening of the system in position C is evident from the rightward shift of the board's resonance peak. The same peak is visible in the impedance plot, highlighting the increased mobility of the exciter when attached to the board.

$\eta \approx 15$ s^{-1} and $K \approx 0.6$ V s m^{-1}. Considering a harmonic input forcing $V(t) = \hat{V}e^{j\omega t}$, one can transform the above in the frequency domain, obtaining:

$$\mathbf{Z}(\omega)\hat{\mathbf{I}} = \hat{\mathbf{V}} \tag{12}$$

where $\hat{\mathbf{I}} = (j\omega\hat{q} := \hat{v}, j\omega\hat{w}, \hat{I})^T$ is the frequency domain current/velocity response; $\hat{\mathbf{V}} = (0, 0, 1)^T$ is the input vector. $\mathbf{Z}(\omega)$ is the 3×3 impedance matrix, not given here for brevity. From the matrix, one can easily get the frequency-domain expressions for the board's response $\hat{v}$ and the electrical impedance $Z := \hat{V}/\hat{I}$. Results are given in Fig. 9, where an excellent match with the experimental results is found.

The model agrees qualitatively and quantitatively with what is observed in Fig. 3, 4, and 6. In particular, note that exciting the board in C yields a stiffening of the first modal frequency in the board's response and the peak shifts to the right, as seen in the experiments summarised in Fig. 4. In the same way, the peaks in the impedance plots change. In particular, placing the exciter in C activates a peak in the transducer's impedance corresponding to the compliant first mode. The same peak is almost completely cancelled when the device is positioned in L1. These results suggest that placing the exciter around a modal maximum may affect the reliability of the measurement procedure, as the actuator does not act as a dead mass but rather as a stiffening device. However, choosing an excitation point away from clear resonances allows obtaining reliable measurements of the board.

References

[1] IEC. Sound system equipment - Part 21: Acoustical (output-based) measurements. 60268-21. International Standard, 2018.

[2] IEC. Sound system equipment - Part 4: Microphones. 60268-4. International Standard, 2018.

[3] AES. AES recommended practice for professional audio - Subjective evaluation of loudspeakers. 20-1996. AES Standard, 2008.

[4] L. Ausiello, L. Yule, G. Squicciarini, and C. Barlow. Guitar soundboard measurements for repeatable acoustic performance manufacturing. In Proceedings Reproduced Sound 2018, Bristol, UK, 27-29 November 2018.

[5] L. Ausiello and V. Hockey. Quantitative measurements to enhance performance of acoustic musical instruments and improve manufacturing. Acoustic Bulletin, 47(2):47–2, 2021.

[6] A. Ausiello, M. Ducceschi, S. Duran, and B. Morrison. Affordable wide-band measurement ecosystem for musical acoustics based on electro-dynamic transducers. Acta Acustica, 8(53):–, 2024.

[7] A. Farina. Simultaneous measurement of impulse response and distortion with a swept-sine technique. In Proceedings of the AES 108 Convention, pages 1–24, Paris, France, 19-22 February 2000.

[8] A. Farina. Advancements in impulse response measurements by sine sweeps. In Proceedings of the AES 122 Convention, pages 1–21, Vienna, Austria, 5-8 May 2007.

[9] P. Guidorzi, L. Barbaresi, D. D'Orazio, and M. Garai. Impulse responses measured with mls or swept-sine signals applied to architectural acoustics: an in-depth analysis of the two methods and some case studies of measurements inside theaters. Energy Procedia, 78:1611–1616, 2015.

[10] F. Policardi. Mls and sine-sweep technique comparison in room-acoustic measurements. Elektrotehniški Vestnik / Electrotechnical Review, 78(3):91–95, 2011.

[11] M. Garai, F. Morandi, D. D'Orazio, S. De Cesaris, and L. Loreti. Acoustic measurements in eleven italian opera houses: Correlations between room criteria and considerations on the local evolution of a typology. Buildings and Environment, 94:900–912, 2015.

[12] N. Thiele. Loudspeakers in vented boxes: Part 1. Journal of the Audio Engineering Society, 19(5):382–392, 1971.

[13] N. Thiele. Loudspeakers in vented boxes: Part 2. Journal of the Audio Engineering Society, 19(6):471–483, 1971.

[14] R. H. Small. Vented-box loudspeaker systems– part 1: Small-signal analysis. Journal of the Audio Engineering Society, 21(5):363–372, 1973.

[15] D. Ponteggia. Loudspeaker electrical impedance measurements methods: A brief review. In International Conference on Noise and Vibration Engineering, pages 1615–1626, Los Angeles, USA, 2006.

[16] N. Giordano. Mechanical impedance of a piano soundboard. The Journal of the Acoustical Society of America, 103(4):2128–2133, 1998.

[17] W. Klippel. Assessment of voice coil peak displacement xmax. In Proceedings of the AES 112 Convention, pages 307–324, Dresden, Germany, 10-13 May 2002.

[18] M. Dodd, W. Klippel, and J. Oclee-Brown. Voice coil impedance as a function of frequency and displacement. In Proceedings of the AES 117th Convention, San Francisco, USA, Oct 2004.

[19] J. Lazar and G. S. Kubota. Analysis of a vented-box loudspeaker system via the impedance function. In Proceedings of the AES 147th Convention, New York, USA, Oct 2019.

[20] R. Magalotti, K. Bugaj, and A. Said. Assessing the acoustic load on a loudspeaker driver through electrical impedance measurements. In Proceedings of the AES Conference, Le Mans, France, Jan 2024.

[21] K. G. McConnell. Vibration Testing: Theory and Practice. John Wiley & Sons, 1995.

[22] P. Varoto and L. de Oliveira. Interaction between a vibration exciter and the structure under test. Sound and Vibration, 36:20–26, 2002.

[23] M. Ducceschi, S. Duran, H. Tahvanainen, and L. Ausiello. A method to estimate the rectangular orthotropic plate elastic constants using least-squares and chladni patterns. Applied Acoustics, 220(109949), 2024.

[24] M. Ducceschi, C. Touzé, S. Bilbao, and C. J. Webb. Nonlinear dynamics of rectangular plates: Investigation of modal interaction in free and forced vibrations. Acta Mechanica, 225(1):213–232, 2014.

[25] Andrea Prato, Alessandro Schiavi, Federico Casassa, et al. A modal approach for reverberation time measurements in non-diffuse sound field. In ICSV23 Proceedings, 2016.